

Diffractive imaging of transient electronic core-shell structures in a nanoplasma

Daniela Rupp,^{1,*} Leonie Flückiger,^{1,2} Marcus Adolph,¹ Tais Gorkhover,^{1,3}
Maria Krikunova,¹ Jan-Phillipe Müller,¹ Maria Müller,¹ Tim Oelze,¹ Yevheniy
Ovcharenko,^{1,4} Mario Sauppe,¹ Sebastian Schorb,¹ David Wolter,¹ Marion
Harmand,⁵ Rolf Treusch,⁵ Christoph Bostedt,^{6,7,†} and Thomas Möller¹

¹*IOAP, Technische Universität Berlin,*

Hardenbergstraße 36, 10623 Berlin, Germany

²*ARC Centre of Excellence for Advanced Molecular Imaging,*

La Trobe University, Bundoora, Victoria 3086, Australia

³*LCLS, SLAC, 2575 Sand Hill Road, Menlo Park, CA 94025, USA*

⁴*European XFEL, DESY, Notkestraße 85, 22603 Hamburg, Germany*

⁵*FLASH, DESY, Notkestraße 85, 22603 Hamburg, Germany*

⁶*Argonne National Laboratory, 9700 S. Cass Avenue, Argonne, IL 60439, USA*

⁷*Department of Physics and Astronomy, Northwestern University,*

2145 Sheridan Road, Evanston, IL 60208, USA

(Dated: November 4, 2016)

Abstract

We have recorded the coherent diffraction images of individual xenon clusters using intense extreme ultraviolet free-electron laser pulses tuned to atomic and ionic resonances in order to elucidate the influence of light induced electronic changes on the diffraction pattern. The data show the emergence of a transient core-shell structure within the otherwise homogeneous sample. Simulations indicate that ionization and nanoplasma formation result in a cluster shell with strongly altered refraction. The presented resonant scattering approach enables the imaging of ultrafast electron dynamics with unprecedented spatial resolution on their natural time scale.

Intense femtosecond short-wavelength pulses from free-electron lasers (FELs) open new avenues to investigate transient states and ultrafast processes with unprecedented spatial and temporal resolution [1–4]. Examples include diverse topics ranging from the first demonstration of femtosecond coherent diffractive imaging [5] and obtaining single-shot 3D information from single nanoparticles [6] to the visualization of ultrafast magnetization dynamics [7], quantum vortices in helium droplets [8], and non-equilibrium dynamics in nanoplasma [9–11].

Typical efforts concentrate on diffractive imaging of the atomic structure or density distribution of the sample. Ultrafast photon induced changes to the sample electronic structure are so far mostly discussed in terms of “damage” in both, experimental [12] and theoretical [13] approaches. However, the availability of intense short-wavelength pulses also yields tremendous opportunity to directly image electronic structure changes with high spatial resolution in a time-resolved manner. During the X-ray scattering process the photons interact with the electrons that are either tightly bound to the nuclei or delocalized in the valence states. In particular near absorption resonances, the X-ray scattering cross section depends sensitively on the wavelength of the incoming photon and the electronic structure of the sample [14, 15].

In this letter we demonstrate how resonant elastic scattering can be used to directly image the spatial distribution of transient charge states in an evolving nanoplasma. As samples we use submicron-sized clusters that are simultaneously transformed to a highly excited nanoplasma and imaged with a single intense femtosecond FEL pulse. On the timescale of the pulse the position of the clusters is frozen in space and ionic motion in the generated nanoplasma can be neglected [16]. Nevertheless, we do observe modulations in the scattering patterns that scale with the FEL intensity and that are characteristic for core-shell structures. As they are independent from the geometric arrangement of the atoms in the cluster, we attribute these modulations to light-induced electronic structure changes which is supported by Mie calculations and Monte-Carlo simulations. The models indicate that the electronic core-shell structures exhibit surprisingly sharp boundaries that act akin to a transient mirror within the nanoplasma. The experiments show the potential of resonant coherent diffractive imaging for taking snapshots of ultrafast ionization dynamics or charge migration in complex samples with femtosecond time and nanometer spatial resolution.

The experiments were performed at the soft X-ray free-electron laser FLASH [17] at 91 eV photon energy (13.6 nm wavelength). The photon energy matches the giant 4d resonance of

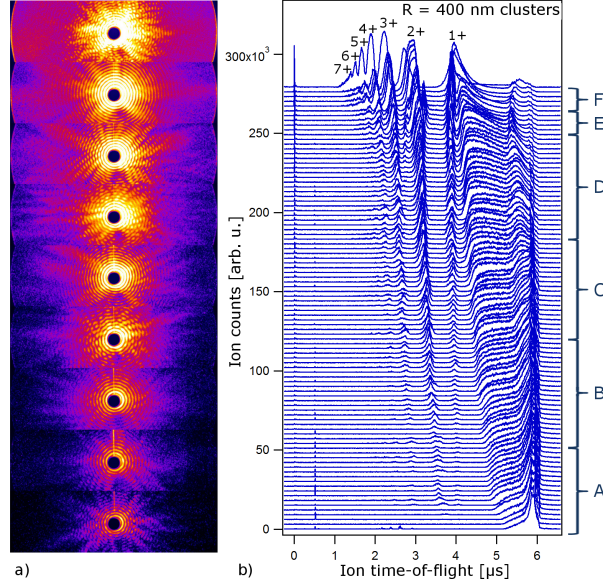


FIG. 1. Individual large xenon clusters irradiated with intense XUV pulses (91 eV photon energy, 10^{14} W/cm² focal power density). All events with single clusters of (400 ± 50) nm radius were selected for analysis (total of 94 events) by the characteristic spacing of the diffraction rings. a) Representative diffraction images, intercepted at different positions of the focal power density distribution. b) Corresponding ion spectra of all 94 events. The average kinetic energy of the Xe^{1+} ions has been used as criterion to sort the events for FEL exposure power density [16], (spectra shifted by an offset for better visibility). For the following analysis, all events were binned into 6 categories A to F according to the abundance of higher charge states (see text and supplemental material [29] for details).

neutral xenon [18] and resonances some Xe charge states [19–24] as discussed in detail below. The roughly 10^{13} photons per pulse were focused into a $20 \mu\text{m}$ (fwhm) spot, reaching power densities up to 5×10^{14} W/cm². The FEL beam intersected a highly diluted jet of very large xenon clusters [25]. An adjustable piezo skimmer slit ensured that only single clusters were in the focus volume per FEL shot [26]. The scattering patterns were measured with a large area scattering detector as previously described [14, 27]. The size of each single, mostly spherical cluster could be determined from the spacing of the extrema in the diffraction patterns [25]. Within the size regime of $R = (400 \pm 50)$ nm a total of 94 diffraction images were obtained. In addition to the diffraction images, coincident single-shot ion spectra were recorded [16, 28].

In Fig. 1a) examples for these single-shot images are displayed. In order to analyze only the intensity dependent changes in the patterns and to cancel out effects from irregular shapes and slightly different sizes of single clusters, all 94 single-cluster measurements within the selected size range were binned into six categories A to F (see brackets on the right side of Fig. 1b) and averaged. Therefore, the 94 data sets were sorted for increasing FEL exposure intensity by the kinetic energy of the Xe^{1+} ions [16], as shown in Fig. 1b) (further details are given in the supplemental material [RefSuppMat]).

The radial profiles resulting from the averaged scattering images of each category A to F are displayed in Fig. 2a). The high-frequency modulation of the profiles reflects the cluster size information. The envelope of profile A, representing the class of clusters exposed to lowest intensities, agrees well with the expected curve for a homogeneous spherical xenon cluster, dropping linearly on a logarithmic scale. In the absence of light induced changes in the particle, the profiles from clusters irradiated with higher FEL intensity would follow a similar curve but with a proportionally higher scattering signal. In contrast, the profile envelopes A to F develop a more and more pronounced lobe structure roughly at 15° to 30° . This superstructure evolving with FEL intensity points to the development of an additional characteristic length scale in the sample. More specifically, the lobe feature is the signature of a core-shell structure with a few tens of nanometer thick outer shell that shows a strongly deviating refractive index compared to the cluster core as will be discussed in more detail below.

A simplifying model allows us to analyze the observed core-shell superstructure with Mie-based simulations: It is assumed that the profiles A to F, obtained at different FEL-intensities, reflect the course of the same evolution, but up to different stages. "Single steps" of the evolution can therefore be extracted from the difference between each two profiles. In Fig. 2b) the difference profiles from Fig 2a) are given (F-E, E-D, and so on). They reveal very distinct features in the superstructure: With increasing FEL intensity a broad lobe appears, becomes more and more pronounced and narrower and shifts towards higher scattering angles.

Simulated profiles matching the core-shell superstructure in Fig. 2b) are shown in Fig. 2c). The simulations were carried out using a code based on Mie theory and extended for spheres with a core-shell structure [30, 32, 33]. A schematic visualization in Fig. 2d) illustrates this evolution. The parameters of the outer shell used in these simulations are given in

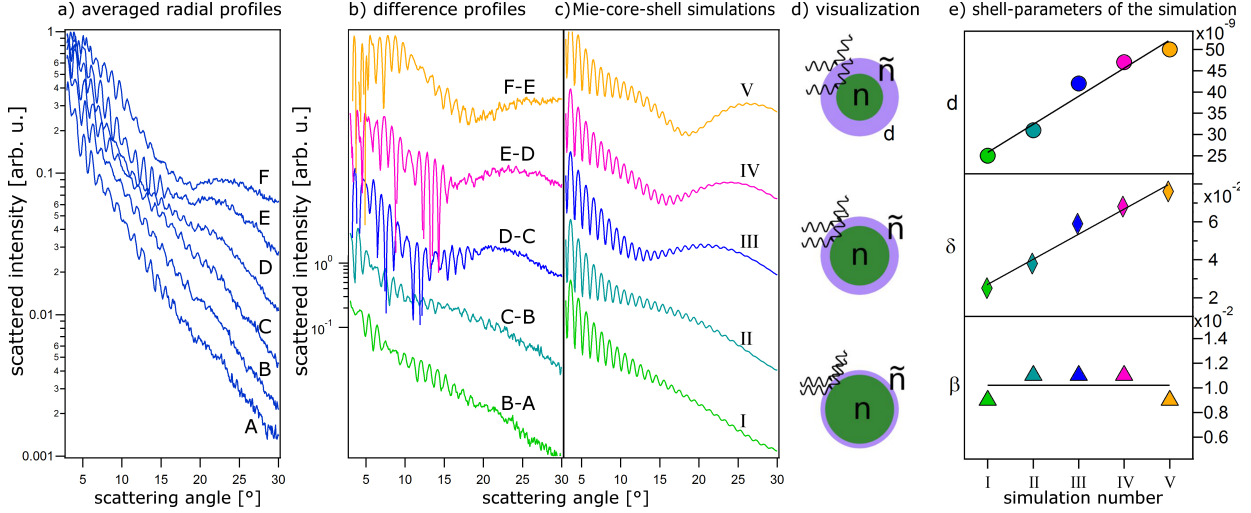


FIG. 2. a) Radial profiles of averaged diffraction images from bins A to F, as indicated in Fig. 1b). The measured scattering intensities are corrected for the flat detector geometry ($I_{sphere} = I_{detect} \cdot \cos \theta^{-3}$ [14]) and the nonlinear detector response ($I_{corr} = I_{sphere}^{2.5}$ [6]), radially averaged and plotted logarithmically vs. scattering angle. Profile A exhibits a ripple structure corresponding to the cluster size on an otherwise linearly dropping (log scale) curve, as expected from Mie theory for a homogeneous xenon cluster. Towards higher exposure power densities up to profile F, an additional large-scale structure evolves. b) The evolution becomes much clearer in the difference profiles from Fig. 2a). For better visibility the curves were shifted by multiplication with a factor. c) Matching calculated profiles obtained with a Mie-based core-shell code [30]. d) Schematic visualization of the spatially inhomogeneous nanoplasma evolving with increasing FEL exposure power density. The beating pattern in the diffraction profiles basically results from the interference of light scattered at the surface and a sharp boundary within the nanoplasma, see discussion in the text. e) Parameters of the shell used as input for the calculations displayed in c), i.e. shell thickness d , refractive index decrement δ (the real part of the refractive index $Re(\tilde{n})$ is given by $1-\delta$), and absorption index β (imaginary part $Im(\tilde{n})$). Black lines serve as guide to the eye. The refractive index of the core was kept constant to $n = 1.007 + i \cdot 0.044$ (values for neutral xenon from [31]).

Fig. 2e), in particular increasing shell thickness, increasing refractive index decrement δ , and a very low absorption coefficient β (factor 4 - 5 less than neutral xenon). Please note that while the tendencies found via the Mie simulations are probably correct, the absolute values might not match the actual optical constants in the nanoplasma because (i) the refractive

index of the core is unknown and (ii) the nanoplasma structure may considerably deviate from a concentric core-shell system. In fact it can be rather expected to be asymmetric in the direction of incident light [34]. Nevertheless, the excellent agreement between Fig. 2b) and c) confirms the basic picture of the phenomenon as a strongly altered outer shell in the cluster nanoplasma. It is notable that the core-shell structure is a general feature because it survives the averaging over many single-cluster patterns which themselves incorporate the average scattering signal over the FEL pulse duration. This raises the question of the origin of this refractive core shell system, i.e. the generation of a tens of nanometers thick outer shell of the nanoplasma with optical properties that differ so drastically from the plasma core.

The origin of the stable core-shell structure may be found in the peculiar electronic properties of xenon atoms and ions in the vicinity of the photon energy of 91 eV. Absorption cross-sections for xenon atoms and atomic ions have been measured [19–24] and are summarized in table I. They reveal a clear step from high to low absorption between Xe^{4+} and Xe^{5+} with extremely high values for the charge state 4+ which exhibits a large ionic resonance at 91 eV. It has to be noted that the atomic/ionic resonances are expected to shift in the plasma environment of the cluster [35], possibly up to several eV [36], as further discussed below. Nevertheless, the atomic absorption cross-sections can be used to gain a first-order picture of the radial charge state distributions: As a model for the light propagation and absorption from cluster surface to core, the charge state densities which are produced in the propagation of an intense 91 eV-pulse through a chain of xenon atoms have been calculated in a basic Monte-Carlo approach for the cross-sections given in table I. The radial density distributions are plotted in figure 3a) for an FEL intensity of $1 \times 10^{14} \text{ W/cm}^2$. We find a good agreement with the results from the Mie-analysis in trend, however not in magnitude (cf. Fig. 2c and e). In particular the ionization model qualitatively explains the radially changing properties with an outer shell of exclusively high charge states that absorb 91 eV

q	neutral	1+	2+	3+	4+	5+	6+	7+
σ [Mbarn]	23	25	22	25	200	<2	<2	<2

TABLE I. Total absorption cross-sections at 91 eV of neutral xenon [19] and xenon charge states 1+ [20], 2+ [21], 3+ [22], 4+ [23], 5 to 7+ [24].

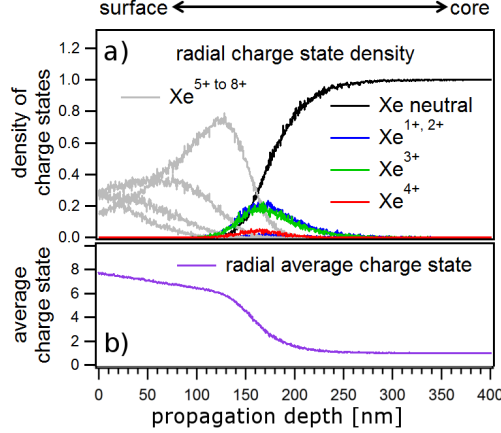


FIG. 3. Simulation of the radially changing a) charge state densities and b) average charge state for a 400 nm radius cluster irradiated with $1 \cdot 10^{14} \text{ W/cm}^2$, corresponding to approximately 870 photons which fall on the geometric cross-section of one xenon atom and propagate into the cluster layer by layer from surface to core. Absorption cross-sections from table 1 were used to calculate the radial charge state densities. Please note that only linear absorption has been taken into account in this simple model, nonlinear effects, light scattering and collisional processes were neglected.

radiation only weakly. As displayed in figure 3b) the abruptly changing absorption cross-sections of xenon charge states result in a step in the average charge state from 6+ to 2+ within approximately 50 nm.

It is important to note, that this rather smooth transition does not suffice to explain the origin of the superstructure in the scattering intensity. To generate pronounced modulations, two preconditions are necessary: (i) a low absorption index in the outer shell and (ii) a *sharp boundary* between regions of different refractive index decrement δ . We have tested this second claim with simple scattering simulations (see supplements for details, method presented in [11]). The modulations would vanish in case of such a smooth transition over several tens of nanometers. We can only speculate about the origin of an abrupt breach of the real part of the refractive index instead of a smooth transition. Our hypothesis is that the radially changing plasma environment of the xenon ions and the resulting, radially changing plasma shift of the resonant energies, might be accountable for this breach, as explained in the following. Xenon charge states with strong absorption resonances in the vicinity of 91 eV (3+ to 6+ [22, 23]) also exhibit strong variations of the real part of the refractive index within

a short energy range. For Xe^{3+} calculations of the atomic scattering factors [37] indicate that between 90 eV and 98 eV the real part of the atomic scattering factor f_1 (proportional to the refractive index decrement δ) changes from high positive to negative values and back several times with peak values of ± 40 . Comparing the radial position of the Xe^{3+} -distribution in figure 3a) (green curve) with the average charge states at the same radial positions, given in figure 3b) (purple curve) clearly shows that the environment of Xe^{3+} ions can be expected to change strongly with radius. Accordingly, this change in the plasma environment may translate into a radially dependent plasma shift of the electronic resonances up to several eV [35], from just below a sharp resonance to just above the resonance. This would result in a drastic change of the real part of the refractive index within a short distance, that would act as a transient mirror. This hypothesis could be tested via detailed modeling beyond the scope of this work.

To summarize, we have presented scattering patterns of single large xenon clusters resonantly excited with intense XUV pulses. They revealed a strong intensity dependent modulation of the scattering distribution, that was analyzed by means of Mie-based simulations for spherical core-shell structures. With rising FEL intensity we find an increasingly thick outer shell characterized by low absorption and a strong and rapid change in refraction. The origin of this abrupt change in refractive index, which is a necessary precondition for modulations, might be connected with the radially changing plasma environment of higher charge states, resulting in a radially changing plasma shift of the electronic resonances. In conclusion, ultrafast light scattering allows for mapping the transient spatial charge distributions of resonant states on nanoscales. This can help to develop a deeper understanding of nanoplasma formation and charge transfer dynamics which play a key role in many areas such as single-shot X-ray imaging, fusion and warm dense matter physics.

The authors want to thank Thomas Fennel and Christian Peltz for helpful and enlightening discussions. Excellent support from IOAP and DESY machine shops is acknowledged. The experiments have received funding from BMBF (grants 05K10KT2/05K13KT2) and DFG (grants BO 3169/2-2 and MO 719/13-1). CB, LF and TG acknowledge funding. M. K. and T. O. acknowledge the financial support by the BMBF project 05K13KT6.

* daniela.rupp@physik.tu-berlin.de

[†] cbostedt@anl.gov

- [1] J. Feldhaus, M. Krikunova, M. Meyer, T. Möller, R. Moshhammer, A. Rudenko, T. Tschentscher, and J. Ullrich, *Journal of Physics B: Atomic, Molecular and Optical Physics* **46**, 164002 (2013).
- [2] C. Bostedt, S. Boutet, D. M. Fritz, Z. Huang, H. J. Lee, H. T. Lemke, A. Robert, W. F. Schlotter, J. J. Turner, and G. J. Williams, *Rev. Mod. Phys.* **88**, 015007 (2016).
- [3] F. Bencivenga, F. Capotondi, E. Principi, M. Kiskinova, and C. Masciovecchio, *Advances in Physics* **63**, 327 (2015).
- [4] M. Yabashi, H. Tanaka, T. Tanaka, H. Tomizawa, T. Togashi, M. Nagasono, T. Ishikawa, J. R. Harries, Y. Hikosaka, A. Hishikawa, K. Nagaya, N. Saito, E. Shigemasa, K. Yamanouchi, and K. Ueda, *Journal of Physics B: Atomic, Molecular and Optical Physics* **46**, 164001 (2013).
- [5] H. N. Chapman, A. Barty, M. J. Bogan, S. Boutet, M. Frank, S. Hau-Riege, S. Marchesini, B. Woods, S. Bajt, W. H. Benner, R. A. London, E. Plonjes, M. Kuhlmann, R. Treusch, S. Dusterer, T. Tschentscher, J. R. Schneider, E. Spiller, T. Möller, C. Bostedt, M. Hoener, D. A. Shapiro, K. O. Hodgson, D. van der Spoel, F. Burmeister, M. Bergh, C. Caleman, G. Huldt, M. Seibert, F. R. N. C. Maia, R. W. Lee, A. Szoke, N. Timneanu, and J. Hajdu, *Nature Physics* **2**, 839 (2006).
- [6] I. Barke, H. Hartmann, D. Rupp, L. Flockiger, M. Sauppe, M. Adolph, S. Schorb, C. Bostedt, R. Treusch, C. Peltz, S. Bartling, T. Fennel, K. Meiwes-Broer, and T. Möller, *Nature Communications* **6**, 6187 (2015).
- [7] C. von Korff Schmising, B. Pfau, M. Schneider, C. M. Günther, M. Giovannella, J. Perron, B. Vodungbo, L. Müller, F. Capotondi, E. Pedersoli, N. Mahne, J. Lüning, and S. Eisebitt, *Phys. Rev. Lett.* **112**, 217203 (2014).
- [8] L. Gomez, K. Ferguson, J. Cryan, C. Bacellar, R. Tanyag, C. Jones, S. Schorb, D. Anielski, A. Belkacem, C. Bernando, R. Boll, J. Bozek, S. Carron, G. Chen, T. Delmas, L. Englert, S. W. Epp, B. Erk, L. Foucar, R. Hartmann, A. Hexemer, M. Huth, J. Kwok, S. R. Leone, J. H. S. Ma, F. R. N. C. Maia, E. Malmerberg, S. Marchesini, D. M. Neumark, B. Poon, J. Prell, D. Rolles, B. Rudek, A. Rudenko, M. Seifrid, K. R. Siefermann, F. P. Sturm, M. Swiggers, J. Ullrich, F. Weise, P. Zwart, C. Bostedt, O. Gessner, and A. F. Vilesov, *Science* **345**, 906 (2014).
- [9] K. R. Ferguson, M. Bucher, T. Gorkhover, S. Boutet, H. Fukuzawa, J. E. Koglin, Y. Kumagai,

- A. Lutman, A. Marinelli, M. Messerschmidt, K. Nagaya, J. Turner, K. Ueda, G. J. Williams, P. H. Bucksbaum, and C. Bostedt, *Science Advances* **2** (2016).
- [10] T. Gorkhover, S. Schorb, R. Coffee, M. Adolph, L. Foucar, D. Rupp, A. Aquila, J. D. Bozek, S. W. Epp, B. Erk, L. Gumprecht, L. Holmegaard, A. Hartmann, R. Hartmann, G. Hauser, P. Holl, A. Hömke, P. Johnsson, N. Kimmel, K.-U. Kühnel, M. Messerschmidt, C. Reich, A. Rouzée, B. Rudek, C. Schmidt, J. Schulz, H. Soltau, S. Stern, G. Weidenspointner, B. White, J. Küpper, L. Strüder, I. Schlichting, J. Ullrich, D. Rolles, A. Rudenko, T. Möller, and C. Bostedt, *Nat Photon* **10**, 93 (2016).
- [11] L. Flückiger, D. Rupp, M. Adolph, T. Gorkhover, M. Krikunova, M. Müller, T. Oelze, Y. Ovcharenko, M. Sauppe, S. Schorb, C. Bostedt, S. Düsterer, M. Harmand, H. Redlin, R. Treusch, and T. Möller, *New Journal of Physics* **18**, 043017 (2016).
- [12] K. Nass, L. Foucar, T. R. M. Barends, E. Hartmann, S. Botha, R. L. Shoeman, R. B. Doak, R. Alonso-Mori, A. Aquila, S. Bajt, A. Barty, R. Bean, K. R. Beyerlein, M. Bublitz, N. Drachmann, J. Gregersen, H. O. Jönsson, W. Kabsch, S. Kassemeyer, J. E. Koglin, M. Krumrey, D. Mattle, M. Messerschmidt, P. Nissen, L. Reinhard, O. Sitsel, D. Sokaras, G. J. Williams, S. Hau-Riege, N. Timneanu, C. Caleman, H. N. Chapman, S. Boutet, and I. Schlichting, *Journal of Synchrotron Radiation* **22**, 225 (2015).
- [13] S.-K. Son, L. Young, and R. Santra, *Phys. Rev. A* **83**, 033402 (2011).
- [14] C. Bostedt, E. Eremina, D. Rupp, M. Adolph, H. Thomas, M. Hoener, A. R. B. de Castro, J. Tiggesbäumker, K.-H. Meiwes-Broer, T. Laarmann, H. Wabnitz, E. Plönjes, R. Treusch, J. R. Schneider, and T. Möller, *Phys. Rev. Lett.* **108**, 093401 (2012).
- [15] B. Wu, T. Wang, C. E. Graves, D. Zhu, W. F. Schlotter, J. J. Turner, O. Hellwig, Z. Chen, H. A. Dürr, A. Scherz, and J. Stöhr, *Phys. Rev. Lett.* **117**, 027401 (2016).
- [16] D. Rupp, L. Flückiger, M. Adolph, T. Gorkhover, M. Krikunova, J. P. Müller, M. Müller, T. Oelze, Y. Ovcharenko, B. Röben, M. Sauppe, S. Schorb, D. Wolter, R. Mitzner, M. Wöstmann, S. Roling, M. Harmand, R. Treusch, M. Arbeiter, T. Fennel, C. Bostedt, and T. Möller, *Phys. Rev. Lett.* **117**, 153401 (2016).
- [17] W. Ackermann *et al.*, *Nature Phot.* **1**, 336 (2007).
- [18] M. Göppert-Mayer, *Phys. Rev.* **60**, 184 (1941).
- [19] D. Ederer and M. Manalis, *J. Opt. Soc. Am.* **65**, 634 (1975).
- [20] Y. Itoh, A. Ito, and M. Kitajima, *Journal of Physics B* **4075**, 3493 (2001).

- [21] P. Andersen, T. Andersen, F. Folkmann, V. Ivanov, H. Kjeldsen, and J. West, *Journal of Physics B* **4075**, 2009 (2009).
- [22] E. Emmons *et al.*, *Physical Review A* **71** (2005).
- [23] A. Aguilar, J. D. Gillaspay, G. F. Gribakin, R. A. Phaneuf, M. F. Gharaibeh, M. G. Kozlov, J. D. Bozek, and A. L. D. Kilcoyne, *Physical Review A* **73**, 1 (2006).
- [24] J. Bizau, J.-M. Esteve, D. Cubaynes, F. J. Wuilleumier, C. Blancard, A. Compant La Fontaine, C. Couillaud, J. Lachkar, R. Marmoret, C. Remond, J. Bruneau, D. Hitz, P. Ludwig, and M. Delaunay, *Physical Review Letters* **84**, 435 (2000).
- [25] D. Rupp, M. Adolph, L. Flückiger, T. Gorkhover, J. P. Müller, M. Müller, M. Sauppe, D. Wolter, S. Schorb, R. Treusch, C. Bostedt, and T. Möller, *J. Chem. Phys.* **141**, 044306 (2014).
- [26] D. Rupp, M. Adolph, , T. Gorkhover, S. Schorb, D. Wolter, R. Hartmann, N. Kimmel, C. Reich, T. Feigl, A. de Castro, R. Treusch, L. Strüder, T. Möller, and C. Bostedt, *New Journal of Physics* **14**, 055016 (2012).
- [27] C. Bostedt, M. Adolph, E. Eremina, M. Hoener, D. Rupp, S. Schorb, H. Thomas, A. de Castro, and T. Möller, *Journal of Physics B: Atomic, Molecular and Optical Physics* **43**, 194011 (2010).
- [28] T. Gorkhover, M. Adolph, D. Rupp, S. Schorb, S. W. Epp, B. Erk, L. Foucar, R. Hartmann, N. Kimmel, K.-U. Kühnel, D. Rolles, B. Rudek, A. Rudenko, R. Andritschke, A. Aquila, J. D. Bozek, N. Coppola, T. Erke, F. Filsinger, H. Gorke, H. Graafsma, L. Gumprecht, G. Hauser, S. Herrmann, H. Hirsemann, A. Hömke, P. Holl, C. Kaiser, F. Krasniqi, J.-H. Meyer, M. Matyssek, M. Messerschmidt, D. Miessner, B. Nilsson, D. Pietschner, G. Potdevin, C. Reich, G. Schaller, C. Schmidt, F. Schopper, C. D. Schröter, J. Schulz, H. Soltau, G. Weidenspointner, I. Schlichting, L. Strüder, J. Ullrich, T. Möller, and C. Bostedt, *Phys. Rev. Lett.* **108**, 245005 (2012).
- [29] Y. f. d. o. . See Supplemental Material at XXXXX, which includes Refs. [XXX, .
- [30] “http://www.scattport.org/www.scattport.org/files/jianqi_shen/,” Web link for the code package by Jianqi Shen for coated spheres (2014).
- [31] “http://henke.lbl.gov/optical_constants/,” Online data base for X-ray optical constants (2016).
- [32] G. Mie, *Annalen der Physik* (1908).
- [33] C. Bohren and D. Huffman, *Absorption and scattering of light by small particles* (John Wiley,

1983).

- [34] C. Peltz, C. Varin, T. Brabec, and T. Fennel, Phys. Rev. Lett. **113**, 133401 (2014).
- [35] S. Hau-Riege, *High-Intensity X-rays – Interaction with Matter* (John Wiley, 2011) pp. 56–57.
- [36] A. Gets and V. Krainov, Journal of Physics B **39**, 1787 (2006).
- [37] J. Nilsen, W. Johnson, and K. Cheng, Proc of SPIE (2007).